ENGINEERING RESEARCH INSTITUTE
UNIVERSITY OF MICHIGAN
ANN ARBOR

MAGNETICALLY SENSITIVE ELECTRICAL RESISTOR MATERIAL

June 1, 1954 to September 30, 1954

ERNST KATZ
Associate Professor of Physics

DEPARTMENT OF THE ARMY
LABORATORY PROCUREMENT OFFICE
U.S. SIGNAL CORPS SUPPLY AGENCY
CONTRACT NO. DA-36-039-sc-52601

November, 1954

ABSTRACT

THEORY

Further progress is reported on a general method being developed for determining the symmetry relations of the bracket quantities for the various crystal symmetries. Results of this method are presented in tables.

EXPERIMENT

Measurements of Bi wires held in a Cardan-suspension are reported as a function of the orientation of the wire defined by the angles ϕ and ψ. Their interpretation is discussed qualitatively, but needs further quantitative elaboration.

Efforts to coat thin films of bismuth on glass by vacuum evaporation are mentioned.

TABLE OF CONTENTS

MAGNETICALLY SENSITIVE ELECTRICAL
RESISTOR MATERIAL

June 1, 1954, to September 30, 1954

A. INTRODUCTION

During the summer months progress has been relatively slow due to vacations, changes in personnel, the moving into larger quarters as a result of the expansion of the contract, and finally because of the design and partial construction of equipment for higher H.

The theoretical efforts have been directed mainly at developing the insight into the symmetry properties of the conductivity tensor components which was begun in the previous reports. This insight is the necessary foundation for enabling us in the near future to interpret the experimental data described in the second part of this report.

The experiments have mostly aimed at measuring for low H the magnetoresistance of bismuth for a sufficiently large number of directions of H with respect to the crystal axes. For low H these data may be described by a magnetoresistance ellipsoid.

A few other miscellaneous experiments with Bi are mentioned.

B. THEORETICAL PART

1. Purpose

In Table V of Report No. 3 some symmetry properties were listed of the bracket quantities describing the dependence of the conductivity components on H. It was stated on page 13 that we wish to derive all the relations among the brackets for all eleven symmetry groups of the reciprocal lattice. This work has been carried essentially to completion and the resulting tables will be useful in all subsequent work for interpreting experimental data.

2. Definitions of the Bracket Symbols and Related Quantities

In order to make the present report more or less self-contained the definition of the bracket symbols is repeated using the same notation as in the previous report.

$$\sigma_{ij} = \sum_{n=0}^{\infty} \sum_{p=0}^{n} \sum_{p'=0}^{n-p} [p',p,n-p-p']_{ij} H_1^{p'} H_2^{p} H_3^{n-p-p'} \qquad (3.3.8)$$

$$[p',p,n-p-p']_{ij} = \int g(E)\nabla E_i \{P[(t\Omega_1)^{p'}(t\Omega_2)^{p}(t\Omega_3)^{n-p-p'}]\} (t\nabla E_j)dk \quad . \qquad (3.3.9)$$

$P[(t\Omega_1)^{p'}(t\Omega_2)^{p}(t\Omega_3)^{n-p-p'}]$ is the sum of all permutations of p' operators $t\Omega_1$, p operators $t\Omega_2$, and n-p-p' operators $t\Omega_3$ in different order. This sum consists of $n!/p!p'!(n-p-p')!$ terms. The definition of the vector operator $\underline{\Omega}$ is

$$\Omega = -(\nabla E x \nabla) \quad , \qquad (4.2.1)$$

which has the transformation properties of an axial vector, i.e., an antisymmetric tensor of the second rank. In order to set this in evidence we shall denote

$$-t\Omega_1 \equiv (13)$$
$$+t\Omega_2 \equiv (23)$$
$$+t\Omega_3 \equiv (12) \quad .$$

The numbers on the right are referred to as "inner indices". From the antisymmetry of the second rank tensor, it follows that interchange of any pair of inner indices within parentheses multiplies the bracket by -1. Only the pairs, (13)(23)(12), will always be used. Furthermore, the outer indices, i, j, shall be denoted as follows:

$11 \equiv \alpha^2$	$12 \equiv \alpha\beta$	$21 \equiv \beta\alpha$	$22 \equiv \beta^2$	(s = 2)
$13 \equiv \alpha\gamma$	$23 \equiv \beta\gamma$	$31 \equiv \gamma\alpha$	$32 \equiv \gamma\beta$	(s = 1)
$33 = \gamma^2$				(s = 0) .

The number of nonthree outer indices will be denoted by s.

3. Outer Symmetry Properties of Brackets

Onsager's relation subjects brackets to some basic symmetry relations, since

$$[p',p,n-p-p']_{ij} = (-)^n [p',p,n-p-p']_{ji} \quad , \qquad (4.4.1)$$

or

Rule I for n = even outer indices may be transposed
Rule II for n = odd transposition of outer indices introduces a - sign
Rule III for n = odd and i = j all brackets vanish.

The relation 4.4.1 will always be used to rewrite brackets with outer indices 32, 13, 21, in terms of brackets with outer indices 23, 13, 12, respectively. Thus, for n = odd only the outer indices 23, 13, 12, occur with s = 1, 2, while for n = even there are in addition 11, 22, 33, with s = 2, 0.

The above rules and relations incorporate the effect of the symmetry due to the inversion center of reciprocal space on the brackets (see also page 12 of the previous report).

4. Transformations Under the Symmetry Operations of Reciprocal Lattices

The eleven crystallographic point groups of reciprocal space can be generated from the following symmetry elements in addition to the inversion center which generates S_2

(a) 2,3,4, or 6 - fold axis along k_3 generating C_{2h}, S_6, C_{4h}, C_{6h},
(b) 2-fold axis along k_1, generating with (a) D_{2h}, D_{3i}, D_{4h}, D_{6h}
(c) 3-fold axis in the (1,1,1) direction generating T_h with D_{2h} and O_h with D_{4h}.

These shall be taken up in order.

5. A Theorem About the Transformation Properties of Brackets Under Rotation About k_3

Consider a transformation consisting of a rotation of the coordinate system about k_3 through an angle ϕ, setting

$$\cos \phi = C$$
$$\sin \phi = S$$

The angle ϕ must be $\pm 2\pi/\mu$, where μ, the multiplicity of the axis must have one of the following values

$$\mu = 2,3,4,6.$$

The transformation matrix connecting new and old coordinates is then

$$\left\| \begin{matrix} C & S & 0 \\ -S & C & 0 \\ 0 & 0 & 1 \end{matrix} \right\| \qquad (4.6.1)$$

In general, any particular bracket in the new coordinate system will be a linear combination of brackets in the old coordinate system. The coefficients of the old, untransformed, brackets in these linear combinations will depend on ϕ. Since for any symmetry operation the result before and after transformation must be indistinguishable, there are in principle as many equations as brackets. However, not all are necessarily independent.

Actually each of the transformed brackets does not involve linear combinations of all untransformed brackets, but only of relatively few. The following rules refer to this. Let

$$p + p' = m \qquad (4.6.2)$$

be the number of inner threes and let 2-s be the number of outer threes.

Rule IV All brackets in a single linear transformation equation have the same n, m, s. This rule is immediately evident from the form of the transformation matrix and the rules of tensor transformation. Thus, for given n, m, s, the number of brackets transforming among themselves is relatively small. It is a matter of simple counting to verify that the number of brackets with the same values of n, m, s is, for

n = odd	s = 1	2(m+1) brackets
	s = 2	(m+1) brackets
n = even	s = 0	(m+1) brackets
	s = 1	2(m+1) brackets
	s = 2	3(m+1) brackets .

The various brackets having the same n, m, s may be considered as the components of a multidimensional Vector. The rotation 4.6.1 in this multidimensional Space is a linear Transformation T of this Vector. By means of a coordinate transformation in this Space, T may be diagonalized and the eigenvectors and eigenvalues found .

Another way of stating the same idea is: Among the brackets with the same n, m, s certain linear combinations can be formed which transform into themselves, multiplied by a constant only. These linear combinations are the eigenvectors; the factors are the eigenvalues.

Under a transformation T corresponding to a rotation (4, 6, 1) which belongs to the group of the reciprocal lattice, any eigenvector must transform identically into itself. This can be achieved in two ways only:

(a) either the eigenvalue = 1,
(b) or the eigenvector = 0.

In the first case no restriction is derived from the rotation for the eigenvector belonging to the eigenvalue 1. The restrictions, imposed by the crystal symmetry on the brackets, find their expression in vanishing eigenvectors belonging to eigenvalues that differ from unity.

It is the purpose at present to lead up to the formulation of the theorem which governs the eigenvalues and eigenvectors. To this end some notations are first introduced. A bracket with given numbers p', p, n will be written with outer indices in the form

$$(\alpha-i\beta)^{z}(\alpha+i\beta)^{s-z}\gamma^{2-s} \quad , \qquad (4.6.3)$$

where z is an integer and $0 \leq z \leq s$. For the various possible values of s and z the meaning of this notation is given in Table I.

TABLE I

THE MEANING OF COMPLEX OUTER INDICES (4.6.3)

s	z	n = odd	n = even
0	0	-	$[\ ]_{33}$
1 1	0 1	$[\ ]_{13} \pm i[\ ]_{23}$	$[\ ]_{13} \pm i[\ ]_{23}$
2 2	0 2	-	$[\ ]_{11} - [\ ]_{22} \pm 2i[\ ]_{12}$
2	1	$2i[\ ]_{12}$	$[\ ]_{11} + [\ ]_{22}$

All brackets have the same p',p,n.

Further, a function F(m,p,w) is defined by the generating equation

$$(1+x)^p(1-x)^{m-p} = \sum_{w=0}^{m} F(m,p,w)x^w \quad , \qquad (4.6.4)$$

where w = 0,1,2, ----m.

It is easily shown that

$$F(m,p,w) = \sum_q (-)^q \binom{p}{w-q} \binom{m-p}{q} \qquad (4.6.5)$$

with q taking integral values from the largest of 0 and w-p up to the smallest of w and m-p. Strictly speaking it is not necessary to limit q in this manner since terms with integral q values outside this range vanish.

The following theorem can now be stated.

Theorem

The eigenvectors corresponding to a transformation of the type (4.6.1) are

$$\sum_{p=o}^{m} i^p \, F(m,p,w) \, [m-p,\ p,\ n-m]_{(\alpha-i\beta)^z(\alpha+i\beta)^{s-z}\gamma^{2-s}} \qquad (4.6.6)$$

(one eigenvector for each pair of w and z).

The eigenvalues are

$$e^{i\phi(m+s-2(w+z))} \quad . \qquad (4.6.7)$$

The proof of this theorem is quite lengthy and will not be given here. The manner in which the theorem is applied should be clear from the foregoing. It enables all the symmetry properties of all the brackets to be written down. This will be done in the next section. We add here one remark in connection with the fact that (4.6.6) is a complex eigenvector. If such an eigenvector is to be zero, this implies two equations, namely, both its real part and its imaginary part must vanish. The conjugate complex eigenvector is then automatically zero and need not be considered separately. Now the complex conjugate of an eigenvector designated by w, z, is the one designated by m-w, s-z. Thus, for the purpose of finding the relations between dependent brackets our attention can be restricted to eigenvectors with either

$$\left.\begin{array}{ll} w \leq m/2 \ ; & z \leq s \\ \text{or} & \\ w \leq m \ ; & z \leq s/2 \ . \end{array}\right\} \qquad (4.6.8)$$

On the other hand, for counting the number of free or independent eigenvectors, which is equal to the number of independent brackets, it is easier to let both w and z run through their entire ranges. It is of interest in this connection to discuss the quantity

$$h \equiv m + s - 2(w+z) \ , \qquad (4.6.9)$$

which ranges from $m + s-2z$ downward in steps of 2; its lowest value being $m + s-2z-2w$. Every time that $h = 0$ or an intergral multiple of μ, (the multiplicity of the k_3 axis), an eigenvector is free. It is not a simple matter to write down in closed form a formula for the number of independent brackets resulting from this prescription for given n and μ So far we have obtained a formula for the case $\mu = 2$. In that case, which has the symmetry C_{2h}, the number of independent eigenvectors or brackets is

$$\left.\begin{array}{ll} \text{for } n = \text{odd} & \dfrac{3n^2 + 10n + 7}{4} \\[2ex] \text{for } n = \text{even} & \dfrac{3n^2 + 10n + 8}{2} \ . \end{array}\right\} \qquad (4.6.10)$$

6. The Dependence Equations Among the Brackets

In this section all the dependence equations between brackets up to $m = 4$ will be derived, and since the method is explained in section 5, the equations for $m > 4$ could be given following the same system.

In order to make the procedure as systematic as possible another rule which is a consequence of the theorem of Section 5 is first stated.

Rule V If $h = m + s - 2(w+z)$ is a

multiple of	2	3	4	6	12	none of these
but not of	3,4	2	3	12		
the vector is restricted for μ =	3,4,6	2,4,6	3,6	4	none	2,3,4,6

Thus, for the first few h-values, the following axes are restricted:

Restrictions for μ =	occur for h =
2,3,4,6	1,5,7,11,13,17,19,23,----
3,4,6	2,10,14,22,----
2,4,6	3,9,15,21,----
3,6	4,8,16,20,----
4	6,18,----
no restrictions	0,12,24,----

In order to apply the theorem, all that is needed is a table of the fuction F(m,p,w). This can easily be constructed if use is made of the following relations that follow directly from the definition (4.6.4).

$$F(m,p,w) = (-)^{m-p}F(m,p,m-w) \qquad (4.7.1)$$

$$\binom{m}{p}F(m,p,w) = (-)^{m-p-w}\binom{m}{w}F(m,m-w,m-p) \qquad (4.7.2)$$

$$F(m,p,w) = (-)^{w}\, F(m,m-p,w) \qquad (4.7.3)$$

$$F(m,p,o) = 1 \qquad (4.7.4)$$

$$F(m,m,w) = \binom{m}{w} \qquad (4.7.5)$$

$$F(m=\text{even},\ p=\text{odd},\ w=m/2) = 0 \qquad (4.7.6)$$

$$F(m=\text{even},\ p=m/2,\ w=\text{odd}) = 0 \qquad (4.7.7)$$

$$F(m,p,w)-F(m,p-1,w)-F(m,p-1,w-1) = F(m,p,w-1) \qquad (4.7.8)$$

Table II lists the values of $i^pF(m,p,w)$. The dotted lines bound the region of p and w from which the remainder of the tables could be obtained by the symmetry formulas (4.7.1) and (4.7.3). These imply that columns are symmetric for even m-p and antisymmetric for odd m-p, and rows are symmetric for even w and antisymmetric for odd w after dividing the numbers first by i^p.

In using this table for finding eigenvectors, it is of course practical to divide each row by any common factor.

With the help of Tables I and II, the eigenvector for any set of values m,w,s,z can now be written. For convenience the inner part of those eigenvectors used in Tables IV and V, i.e., the part which follows from m and w without reference to the outer part which follows from s and z according to Table I, has been explicitly listed in Table III.

TABLE II

THE FUNCTION $i^p F(m,p,w)$

m = 0 $p = p' = w = 0$ $i^0 F(0,0,0) = 1$

m = 1

w \ p	0	1
0	1	i
1	-1	i

m = 2

w \ p	0	1	2
0	1	i	-1
1	-2	0	-2
2	1	-i	-1

m = 3

w \ p	0	1	2	3
0	1	i	-1	-i
1	-3	-i	-1	-3i
2	3	-i	1	-3i
3	-1	i	1	-i

m = 4

w \ p	0	1	2	3	4
0	1	i	-1	-i	1
1	-4	-2i	0	-2i	4
2	6	0	2	0	6
3	-4	2i	0	2i	4
4	1	-i	-1	i	1

etc.

TABLE III

INNER PARTS OF EIGENVECTORS FOR VARIOUS m, w

m	w	Inner Part of Eigenvector
0	0	[0,0,n]
1	0	([1,0,n-1] + i[0,1,n-1])
2	0	([2,0,n-2] + i[1,1,n-2] - [0,2,n-2])
2	1	([2,0,n-2] + [0,2,n-2])
3	0	([3,0,n-3] + i[2,1,n-3] - [1,2,n-3] - i[0,3,n-3])
3	1	(3[3,0,n-3] + i[2,1,n-3] + [1,2,n-3] + 3i[0,3,n-3])
4	0	([4,0,n-4] + i[3,1,n-3] - [2,2,n-4] - i[1,3,n-4]) + [0,4,n-4])
4	1	(2[4,0,n-4] + i[3,1,n-4] + i[1,3,n-4] - 2[0,4,n-4])
4	2	(3[4,0,n-4] + [2,2,n-4] + 3[0,4,n-4])

All the bracket relations can now be listed. This is done in Tables IV and V. The tables are divided into n = odd (Table IV) and n = even (Table V). In the first four columns the sets of values of m, s, w, and z are listed. Now a pair of such sets, m, s, w, z and m,s, m-w,s-z, give conjugate complex eigenvectors. Therefore, only one set of such a pair has been listed; namely the one corresponding to nonnegative h. The two sets of each pair correspond to equal and opposite h values.

The next column lists h. The sets of m, s, w, z are arranged so as to have together those h values which correspond to equations for the same axis orders, μ, listed in the last column. The order is further determined by Rule V. First, sets with h = 0, or a multiple of 12, yielding no equations are listed; then the sets with restrictions for μ = 2,3,4,6; then for μ = 3,4,6,etc., as indicated in the example given under Rule V.

The next column lists the equations that follow from setting the eigenvectors corresponding to the set m, w, s, z equal to zero; the last column indicates for which values of μ these equations are valid. Whenever justified, later equations use the results of earlier ones in order to obtain their simplest form. Equations of earlier lines, which may be disregarded because they appear later in simpler form, can be recognized by parentheses around the corresponding μ values. For example, in Table IV the case (m,s,w,z) = (2,1,1,0) results in two equations which are of interest for μ = 3; whereas, for μ = 2, 4, 6 the results of this line may be disregarded since they have been combined with the results of (m,w,s,z) = (2,0,1,0). On the line of the latter, the combined results of both sets are listed in their simplest form.

As before, an arbitrary odd number is denoted by ω and an arbitrary even number by ϵ. We have discussed in detail the way in which these tables are constructed in order to permit easy checking of the relations presented.

TABLE IV

BRACKET RELATIONS FOR n = ODD, m = 0, 1, 2, 3

m	w	s	z	h	Equations	μ
0	0	2	1	0	-	-
0	0	1	0	1	$[00\omega]_{13} = [00\omega]_{23} = 0$	2346
1	0	1	1	0	-	-
1	0	2	1	1	$[10\epsilon]_{12} = [01\epsilon]_{12} = 0$	2346
1	0	1	0	2	$[10\epsilon]_{13} = [01\epsilon]_{23}$	346
					$[10\epsilon]_{23} = -[01\epsilon]_{13}$	346
2	1	2	1	0	-	-
2	1	1	0	1	$[20\omega]_{13} = -[02\omega]_{13} = -\frac{1}{2}[11\omega]_{23}$	(2)3(46)
2	0	1	1	1	$[20\omega]_{23} = -[02\omega]_{23} = \frac{1}{2}[11\omega]_{13}$	(2)3(46)
2	0	2	1	2	$[11\omega]_{12} = 0$	346
					$[20\omega]_{12} = [02\omega]_{12}$	346
2	0	1	0	3	$[20\omega]_{13} = [02\omega]_{13} = [11\omega]_{13} = 0$	246
					$[20\omega]_{23} = [02\omega]_{23} = [11\omega]_{23} = 0$	246
3	1	1	1	0	-	-
3	1	2	1	1	$3[30\epsilon]_{12} = -[12\epsilon]_{12}$	(2)3(46)
					$3[03\epsilon]_{12} = -[21\epsilon]_{12}$	(2)3(46)
3	1	1	0	2	$[30\epsilon]_{13} = [03\epsilon]_{23}$	(3)4(6)
3	0	1	1	2	$[30\epsilon]_{23} = -[03\epsilon]_{13}$	(3)4(6)
					$[21\epsilon]_{23} = [12\epsilon]_{13}$	(3)4(6)
					$[21\epsilon]_{13} = -[12\epsilon]_{23}$	(3)4(6)
3	0	2	1	3	$[30\epsilon]_{12} = [03\epsilon]_{12} = [21\epsilon]_{12} = [12\epsilon]_{12} = 0$	246
3	0	1	0	4	$[30\epsilon]_{13} = [03\epsilon]_{23} = [21\epsilon]_{23} = [12\epsilon]_{13}$	36
					$[30\epsilon]_{23} = -[03\epsilon]_{13} = -[21\epsilon]_{13} = [12\epsilon]_{23}$	36

TABLE V

BRACKET RELATIONS FOR n = EVEN, m = 0, 1, 2, 3

m	w	s	z	h	Equations	μ
0	0	0	0	0	-	-
0	0	2	1	0	-	-
0	0	1	0	1	$[00\epsilon]_{13} = [00\epsilon]_{23} = 0$	2346
0	0	2	0	2	$[00\epsilon]_{11} = [00\epsilon]_{22}$	346
					$[00\epsilon]_{12} = 0$	346
1	0	1	1	0	-	-
1	0	0	0	1	$[10\omega]_{33} = [01\omega]_{33} = 0$	2346
1	0	2	1	1 }	$[10\omega]_{11} = -[10\omega]_{22} = -[01\omega]_{12}$	(2)3(46)
1	1	2	0	1 }	$[01\omega]_{11} = -[01\omega]_{22} = [10\omega]_{12}$	(2)3(46)
1	0	1	0	2	$[10\omega]_{13} = [01\omega]_{23}$	346
					$[10\omega]_{23} = -[01\omega]_{13}$	346
1	0	2	0	3	$[10\omega]_{11} = [10\omega]_{22} = [10\omega]_{12} = [01\omega]_{11} =$ $= [01\omega]_{22}\ [01\omega]_{12} = 0$	246
2	1	2	1	0	-	-
2	1	0	0	0	-	-
2	0	2	2	0	-	-
2	1	1	0	1 }	$2[20\epsilon]_{13} = -2[02\epsilon]_{13} = -[11\epsilon]_{23}$	(2)3(46)
2	0	1	1	1 }	$2[20\epsilon]_{23} = -2[02\epsilon]_{23} = [11\epsilon]_{13}$	(2)3(46)
2	0	2	1	2 }	$[20\epsilon]_{11} = [02\epsilon]_{22}$	346
2	1	2	0	2 }	$[02\epsilon]_{11} = [20\epsilon]_{22}$	346
					$[20\epsilon]_{12} = -[02\epsilon]_{12}$	346
					$[11\epsilon]_{11} = -[11\epsilon]_{22}$	346
2	0	0	0	2	$[20\epsilon]_{33} = [02\epsilon]_{33}$	346
					$[11\epsilon]_{33} = 0$	346
2	0	1	0	3	$[20\epsilon]_{13} = [20\epsilon]_{23} = [02\epsilon]_{13} = [02\epsilon]_{23} = 0$	246
					$[11\epsilon]_{13} = [11\epsilon]_{23} = 0$	246
2	0	2	0	4	$[11\epsilon]_{12} = [20\epsilon]_{11} - [20\epsilon]_{22}$	36
					$2[20\epsilon]_{12} = -[11\epsilon]_{11} = [11\epsilon]_{22}$	36
3	1	1	1	0	-	-
3	1	0	0	1	$3[30\omega]_{33} = -[12\omega]_{33}$	(2)3(46)
					$3[03\omega]_{33} = -[21\omega]_{33}$	(2)3(46)

TABLE V (continued)

BRACKET RELATIONS FOR n = EVEN, m = 3, 4

m	w	s	z	h	Equations	μ
3	1	2	1	1	$2[21\omega]_{12} = -[30\omega]_{11} + [30\omega]_{22} =$	
					$= -[12\omega]_{11} + [12\omega]_{22} = 2[03\omega]_{12}$	(2)3(46)
3	2	2	0	1	$2[12\omega]_{12} = [03\omega]_{11} - [03\omega]_{22} =$	
					$= [21\omega]_{11} - [21\omega]_{22} = 2[30\omega]_{12}$	(2)3(46)
3	0	2	2	1	$2[30\omega]_{11} + [30\omega]_{22} + [12\omega]_{22} = 0$	(2)3(46)
3	0	2	0	5	$2(03\omega]_{11} + [03\omega]_{22} + [21\omega]_{22} = 0$	(2)3(46)
3	1	1	0	2	$[30\omega]_{13} = [03\omega]_{23}$	(3)4(6)
3	0	1	1	2	$[30\omega]_{23} = -[03\omega]_{13}$	(3)4(6)
					$[12\omega]_{13} = [21\omega]_{23}$	(3)4(6)
					$[12\omega]_{23} = -[21\omega]_{13}$	(3)4(6)
3	1	2	0	3	$[30\omega]_{11} = [30\omega]_{22} = [30\omega]_{12} = 0$	246
					$[03\omega]_{11} = [03\omega]_{22} = [03\omega]_{12} = 0$	246
3	0	2	1	3	$[12\omega]_{11} = [12\omega]_{22} = [12\omega]_{12} = [21\omega]_{11} =$	
					$= [21\omega]_{22} = [21\omega]_{12} = 0$	246
3	0	0	0	3	$[30\omega]_{33} = [21\omega]_{33} = [12\omega]_{33} = [03\omega]_{33} = 0$	246
3	0	1	0	4	$[30\omega]_{13} = [21\omega]_{23} = [12\omega]_{13} = [03\omega]_{23}$	36
					$[30\omega]_{23} = -[21\omega]_{13} = [12\omega]_{23} = -[03\omega]_{13}$	36
4	2	2	1	0	-	-
4	2	0	0	0	-	-
4	1	2	2	0	-	-
4	2	1	0	1	$3[40\epsilon]_{13} + [22\epsilon]_{13} + 3[04\epsilon]_{13} = 0$	(2)3(46)
					$3[40\epsilon]_{23} + [22\epsilon]_{23} + 3[04\epsilon]_{23} = 0$	(2)3(46)
4	1	1	1	1	$2[40\epsilon]_{13} + [31\epsilon]_{23} + [13\epsilon]_{23} - 2[04\epsilon]_{13} = 0$	(2)3(46)
4	0	1	0	5	$2[40\epsilon]_{23} - [31\epsilon]_{13} - [13\epsilon]_{13} - 2[04\epsilon]_{23} = 0$	(2)3(46)
					$4[40\epsilon]_{13} - [31\epsilon]_{23} + [13\epsilon]_{23} + 4[04\epsilon]_{13} = 0$	(2)3(46)
					$4[40\epsilon]_{23} + [31\epsilon]_{13} - [13\epsilon]_{13} + 4[04\epsilon]_{23} = 0$	(2)3(46)
4	2	2	0	2	Simpler forms below	(346)
4	1	2	1	2	Simpler forms below	(346)
4	1	0	0	2	$[40\epsilon]_{33} = [04\epsilon]_{33}$; $[31\epsilon]_{33} = -[13\epsilon]_{33}$	(3)4(6)
4	0	2	2	2	Simpler forms below	(346)
4	1	1	0	3	$[40\epsilon]_{13} = [40\epsilon]_{23} = [31\epsilon]_{13} = [31\epsilon]_{23} = 0$	246
					$[22\epsilon]_{13} = [22\epsilon]_{23} = 0$	246
4	0	1	1	3	$[04\epsilon]_{13} = [04\epsilon]_{23} = [13\epsilon]_{13} = [13\epsilon]_{23} = 0$	246

TABLE V (continued)

BRACKET RELATIONS FOR n = EVEN, m = 4

m	w	s	z	h	Equations	μ
4	1	2	0	4	$[31\epsilon]_{11} = -[31\epsilon]_{22}$	36
4	0	2	1	4	$[13\epsilon]_{11} = -[13\epsilon]_{22}$	36
					$2[40\epsilon]_{11} - 2[04\epsilon]_{11} = [31\epsilon]_{12} + [13\epsilon]_{12}$	36
					$2[40\epsilon]_{11} + 2[40\epsilon]_{22} = [22\epsilon]_{11} + [22\epsilon]_{22} =$	
					$= 2[04\epsilon]_{11} + 2[04\epsilon]_{22}$	36
					$-3[13\epsilon]_{12} + 3[31\epsilon]_{12} = 2[22\epsilon]_{11} - 2[22\epsilon]_{22} =$	
					$= 12[40\epsilon]_{22} - 12[04\epsilon]_{11}$	36
					$-8[40\epsilon]_{12} = 3[13\epsilon]_{11} + [31\epsilon]_{11}$	36
					$8[04\epsilon]_{12} = [13\epsilon]_{11} + 3[31\epsilon]_{11}$	36
					$-[22\epsilon]_{12} = 3[40\epsilon]_{12} + 3[04\epsilon]_{12}$	36
4	0	0	0	4	$[40\epsilon]_{33} + [04\epsilon]_{33} = [22\epsilon]_{33}$	36
					$[31\epsilon]_{33} = [13\epsilon]_{33} = 0$	36
4	0	2	0	6	$[40\epsilon]_{11} = [04\epsilon]_{22}$	4
					$[40\epsilon]_{22} = [04\epsilon]_{11}$	4
					$[22\epsilon]_{11} = [22\epsilon]_{22}$	4
					$[31\epsilon]_{12} = [13\epsilon]_{12}$	4
					$[40\epsilon]_{12} = -[04\epsilon]_{12}$	4
					$[22\epsilon]_{12} = 0$	4
					$[31\epsilon]_{11} = -[13\epsilon]_{22}$	4
					$[31\epsilon]_{22} = -[13\epsilon]_{11}$	4

7. The Tables of Brackets for the Eleven Classes

Using the results of Tables IV and V, the brackets up to n = 4, can be tabulated for S_2, C_{2h}, S_6, C_{4h}, C_{6h}. In order to add the effect of a twofold axis along k_1, the results for C_{2h} are subjected to a permutation $3 \to 1$, $1 \to 2$, $2 \to 3$. Combining the results of this permutation, which only indicates an additional number of zeros, with the results of the above classes the table of brackets is obtained for D_{2h}, D_{3i}, D_{4h}, D_{6h}. Finally, in order to obtain the results for T_h and O_h, the results of D_{2h} and D_{4h} were (mentally) subjected to the same permutation, this time equating all the results before and after permutation (not only the zeros). It is convenient to use here the easily proved rule that if in any bracket written in the form $[(23)^p(31)^{p'}(12)^{n-p-p'}]_{ij}$, at least one of the numbers 1, 2, 3 occurs an odd number of times (inside and outside counted together), the bracket vanishes under this permutation.

In this way Table VI has been constructed. On each page the bracket symbols for one class are listed. S_2 is not listed since all brackets are arbitrary except those which vanish due to (4.4.1). The number of independent brackets for each value of n is listed in the second column; the inside of the brackets is listed in the third column; the outer indices are listed horizontally in the remaining six columns. In cases where one bracket is expressible in terms of one or more others, a choice of independent ones has been made that leads to the simplest expressions of interdependence.

In order to see all the dependences, it is important to observe where a symbol is found in the tables. For example, for C_{4h} we find the symbol $[200]_{11}$ at the place $[200]_{11}$ and at the place $[200]_{22}$, signifying that $[200]_{22} = [200]_{11}$. Thus, if a symbol occupies its own place it is chosen independently; if it occupies another place it is dependent.

The tables will be used in the next report for interpreting the measurements on Bismuth (class D_{3i}). They represent, for the field of magnetoresistance and Hall effect, the equivalent of Voigt's well-known tables for the elastic moduli.

TABLE VI

THE BRACKET SYMBOLS UP TO n = 4, FOR C_{2h}

		ij	11	22	33	23	31	12
n=0	4	[000]	$[000]_{11}$	$[000]_{22}$	$[000]_{33}$	0	0	$[000]_{12}$
n=1	5	[100]	0	0	0	$[100]_{23}$	$[100]_{31}$	0
		[010]	0	0	0	$[010]_{23}$	$[010]_{31}$	0
		[001]	0	0	0	0	0	$[001]_{12}$
n=2	20	[200]	$[200]_{11}$	$[200]_{22}$	$[200]_{33}$	0	0	$[200]_{12}$
		[020]	$[020]_{11}$	$[020]_{22}$	$[020]_{33}$	0	0	$[020]_{12}$
		[002]	$[002]_{11}$	$[002]_{22}$	$[002]_{33}$	0	0	$[002]_{12}$
		[011]	0	0	0	$[011]_{23}$	$[011]_{31}$	0
		[101]	0	0	0	$[101]_{23}$	$[101]_{31}$	0
		[110]	$[110]_{11}$	$[110]_{22}$	$[110]_{33}$	0	0	$[110]_{12}$
n=3	16	[300]	0	0	0	$[300]_{23}$	$[300]_{31}$	0
		[030]	0	0	0	$[030]_{23}$	$[030]_{31}$	0
		[003]	0	0	0	0	0	$[003]_{12}$
		[012]	0	0	0	$[012]_{23}$	$[012]_{31}$	0
		[021]	0	0	0	0	0	$[021]_{12}$
		[102]	0	0	0	$[102]_{23}$	$[102]_{31}$	0
		[201]	0	0	0	0	0	$[201]_{12}$
		[120]	0	0	0	$[120]_{23}$	$[120]_{31}$	0
		[210]	0	0	0	$[210]_{23}$	$[210]_{31}$	0
		[111]	0	0	0	0	0	$[111]_{12}$
n=4	48	[400]	$[400]_{11}$	$[400]_{22}$	$[400]_{33}$	0	0	$[400]_{12}$
		[040]	$[040]_{11}$	$[040]_{22}$	$[040]_{33}$	0	0	$[040]_{12}$
		[004]	$[004]_{11}$	$[004]_{22}$	$[004]_{33}$	0	0	$[003]_{12}$
		[013]	0	0	0	$[013]_{23}$	$[013]_{31}$	0
		[031]	0	0	0	$[031]_{23}$	$[031]_{31}$	0
		[103]	0	0	0	$[103]_{23}$	$[103]_{31}$	0
		[301]	0	0	0	$[301]_{23}$	$[301]_{31}$	0
		[130]	$[130]_{11}$	$[130]_{22}$	$[130]_{33}$	0	0	$[130]_{12}$
		[310]	$[310]_{11}$	$[310]_{22}$	$[310]_{33}$	0	0	$[310]_{12}$
		[022]	$[022]_{11}$	$[022]_{22}$	$[022]_{33}$	0	0	$[022]_{12}$
		[202]	$[202]_{11}$	$[202]_{22}$	$[202]_{33}$	0	0	$[202]_{12}$
		[220]	$[220]_{11}$	$[220]_{22}$	$[220]_{33}$	0	0	$[220]_{12}$
		[211]	0	0	0	$[211]_{23}$	$[211]_{31}$	0
		[121]	0	0	0	$[121]_{23}$	$[121]_{31}$	0
		[112]	$[112]_{11}$	$[112]_{22}$	$[112]_{33}$	0	0	$[112]_{12}$

TABLE VI (continued)

THE BRACKET SYMBOLS, UP TO n = 4, FOR S_6

		ij	11	22	33	23	31	12
n=0	2	[000]	$[000]_{11}$	$[000]_{11}$	$[000]_{33}$	0	0	0
n=1	3	[100]	0	0	0	$[100]_{23}$	$-[010]_{23}$	0
		[010]	0	0	0	$[010]_{23}$	$[100]_{23}$	0
		[001]	0	0	0	0	0	$[001]_{12}$
n=2	12	[200]	$[200]_{11}$	$[200]_{22}$	$[200]_{33}$	$[200]_{23}$	$[200]_{31}$	$[200]_{12}$
		[020]	$[200]_{22}$	$[200]_{11}$	$[200]_{33}$	$-[200]_{23}$	$-[200]_{31}$	$-[200]_{12}$
		[002]	$[002]_{11}$	$[002]_{11}$	$[002]_{33}$	0	0	0
		[011]	$[011]_{11}$	$-[011]_{11}$	0	$[011]_{23}$	$[011]_{31}$	$-[101]_{11}$
		[101]	$[101]_{11}$	$-[101]_{11}$	0	$-[011]_{31}$	$[011]_{23}$	$[011]_{11}$
		[110]	$-2[200]_{12}$	$2[200]_{12}$	0	$-2[200]_{31}$	$2[200]_{23}$	$[200]_{11}-[200]_{22}$
n=3	10	[300]	0	0	0	$[300]_{23}$	$[300]_{31}$	$[300]_{12}$
		[030]	0	0	0	$-[300]_{31}$	$[300]_{23}$	$[030]_{12}$
		[003]	0	0	0	0	0	$[003]_{12}$
		[012]	0	0	0	$[012]_{23}$	$[012]_{31}$	0
		[021]	0	0	0	$[021]_{23}$	$[021]_{31}$	$[021]_{12}$
		[102]	0	0	0	$[012]_{31}$	$-[012]_{23}$	0
		[201]	0	0	0	$-[021]_{23}$	$-[021]_{31}$	$[021]_{12}$
		[120]	0	0	0	$[300]_{23}$	$[300]_{31}$	$-3[300]_{12}$
		[210]	0	0	0	$-[300]_{31}$	$[300]_{23}$	$-3[030]_{12}$
		[111]	0	0	0	$-2[021]_{31}$	$2[021]_{23}$	0
n=4	30	[400]	$[400]_{11}$	$[400]_{22}$	$[400]_{33}$	$[400]_{23}$	$[400]_{31}$	$-\frac{1}{8}\{[310]_{11}+3[130]_{11}\}$
		[040]	$[040]_{11}$	$[400]_{11}+[400]_{22}-[040]_{11}$	$[400]_{33}$	$[040]_{23}$	$[040]_{31}$	$\frac{1}{8}\{[310]_{11}+[130]_{11}\}$
		[004]	$[004]_{11}$	$[004]_{11}$	$[004]_{33}$	0	0	0
		[013]	$[013]_{11}$	$-[013]_{11}$	0	$[013]_{23}$	$[013]_{31}$	$-[103]_{11}$
		[031]	$[031]_{11}$	$[031]_{11}-2[301]_{12}$	$[031]_{33}$	$[031]_{23}$	$[031]_{31}$	$[031]_{12}$
		[103]	$[103]_{11}$	$-[103]_{11}$	0	$-[013]_{31}$	$[013]_{23}$	$[013]_{11}$
		[301]	$[301]_{11}$	$[301]_{11}+2[031]_{12}$	$[301]_{33}$	$-[031]_{31}$	$[031]_{23}$	$[301]_{12}$
		[130]	$[130]_{11}$	$-[130]_{11}$	0	$-3[400]_{31}-[040]_{31}$	$3[400]_{23}+[040]_{23}$	$[400]_{11}-2[400]_{22}+[040]_{11}$
		[310]	$[310]_{11}$	$-[310]_{11}$	0	$[400]_{31}+3[040]_{31}$	$-[400]_{23}-3[040]_{23}$	$[400]_{11}+2[400]_{22}-3[040]_{11}$
		[022]	$[202]_{22}$	$[202]_{11}$	$[202]_{33}$	$-[202]_{23}$	$-[202]_{31}$	$-[202]_{12}$
		[202]	$[202]_{11}$	$[202]_{22}$	$[202]_{33}$	$[202]_{23}$	$[202]_{31}$	$[202]_{12}$
		[220]	$[400]_{11}+4[400]_{22}-3[040]_{11}$	$[400]_{11}-2[400]_{22}+3[040]_{11}$	$2[400]_{33}$	$-3\{[400]_{23}+[040]_{23}\}$	$-3\{[400]_{31}+[040]_{31}\}$	$-\frac{3}{4}\{[310]_{11}-[130]_{11}\}$
		[211]	$-3[031]_{11}+4[301]_{12}$	$-3[031]_{11}+2[301]_{12}$	$-3[031]_{33}$	$[031]_{23}$	$[031]_{31}$	$[031]_{12}$
		[121]	$-3[301]_{11}-4[031]_{12}$	$-3[301]_{11}-2[031]_{12}$	$-3[301]_{33}$	$-[031]_{31}$	$[031]_{23}$	$[301]_{12}$
		[112]	$-2[202]_{12}$	$2[202]_{12}$	0	$-2[202]_{31}$	$2[202]_{23}$	$[202]_{11}-[202]_{22}$

TABLE VI (continued)

THE BRACKET SYMBOLS UP TO n = 4, FOR C_{4h}

		ij	11	22	33	23	31	12
n=0	2	[000]	$[000]_{11}$	$[000]_{11}$	$[000]_{33}$	0	0	0
n=1	3	[100]	0	0	0	$[100]_{23}$	$[100]_{31}$	0
		[010]	0	0	0	$-[100]_{31}$	$[100]_{23}$	0
		[001]	0	0	0	0	0	$[001]_{12}$
n=2	10	[200]	$[200]_{11}$	$[200]_{22}$	$[200]_{33}$	0	0	$[200]_{12}$
		[020]	$[200]_{22}$	$[200]_{11}$	$[200]_{33}$	0	0	$-[200]_{12}$
		[002]	$[002]_{11}$	$[002]_{11}$	$[002]_{33}$	0	0	0
		[011]	0	0	0	$[011]_{23}$	$[011]_{31}$	0
		[101]	0	0	0	$-[011]_{31}$	$[011]_{23}$	0
		[110]	$[110]_{11}$	$-[110]_{11}$	0	0	0	$[110]_{12}$
n=3	8	[300]	0	0	0	$[300]_{23}$	$[300]_{31}$	0
		[030]	0	0	0	$-[300]_{31}$	$[300]_{23}$	0
		[003]	0	0	0	0	0	$[003]_{12}$
		[012]	0	0	0	$[012]_{23}$	$[012]_{31}$	0
		[021]	0	0	0	0	0	$[021]_{12}$
		[102]	0	0	0	$[012]_{31}$	$-[012]_{23}$	0
		[201]	0	0	0	0	0	$[021]_{12}$
		[120]	0	0	0	$[120]_{23}$	$[120]_{31}$	0
		[210]	0	0	0	$-[120]_{31}$	$[120]_{23}$	0
		[111]	0	0	0	0	0	0
n=4	24	[400]	$[400]_{11}$	$[400]_{22}$	$[400]_{33}$	0	0	$[400]_{12}$
		[040]	$[400]_{22}$	$[400]_{11}$	$[400]_{33}$	0	0	$-[400]_{12}$
		[004]	$[004]_{11}$	$[004]_{11}$	$[004]_{33}$	0	0	0
		[013]	0	0	0	$[013]_{23}$	$-[103]_{23}$	0
		[031]	0	0	0	$[031]_{23}$	$[031]_{31}$	0
		[103]	0	0	0	$[103]_{23}$	$[013]_{23}$	0
		[301]	0	0	0	$-[031]_{31}$	$[031]_{23}$	0
		[130]	$-[310]_{22}$	$-[310]_{11}$	$[130]_{33}$	0	0	$[130]_{12}$
		[310]	$[310]_{11}$	$[310]_{22}$	$-[130]_{33}$	0	0	$[130]_{12}$
		[022]	$[202]_{22}$	$[202]_{11}$	$[202]_{33}$	0	0	$[022]_{12}$
		[202]	$[202]_{11}$	$[202]_{22}$	$[202]_{33}$	0	0	$-[022]_{12}$
		[220]	$[220]_{11}$	$[220]_{11}$	$[220]_{33}$	0	0	0
		[211]	0	0	0	$[211]_{23}$	$[211]_{31}$	0
		[121]	0	0	0	$-[211]_{31}$	$[211]_{23}$	0
		[112]	$[112]_{11}$	$-[112]_{11}$	0	0	0	$[112]_{12}$

TABLE VI (continued)

THE BRACKET SYMBOLS, UP TO n = 4, FOR C_{6h}

		ij	11	22	33	23	31	12
n=0	2	[000]	$[000]_{11}$	$[000]_{11}$	$[000]_{33}$	0	0	0
n=1	3	[100]	0	0	0	$[100]_{23}$	$[100]_{31}$	0
		[010]	0	0	0	$-[100]_{31}$	$[100]_{23}$	0
		[001]	0	0	0	0	0	$[001]_{12}$
n=2	8	[200]	$[200]_{11}$	$[200]_{22}$	$[200]_{33}$	0	0	$[200]_{12}$
		[020]	$[200]_{22}$	$[200]_{11}$	$[200]_{33}$	0	0	$-[200]_{12}$
		[002]	$[002]_{11}$	$[002]_{11}$	$[002]_{33}$	0	0	0
		[011]	0	0	0	$[011]_{23}$	$[011]_{31}$	0
		[101]	0	0	0	$-[011]_{31}$	$[011]_{23}$	0
		[110]	$-2[200]_{12}$	$2[200]_{12}$	0	0	0	$[200]_{11}-[200]_{22}$
n=3	6	[300]	0	0	0	$[300]_{23}$	$[300]_{31}$	0
		[030]	0	0	0	$-[300]_{31}$	$[300]_{23}$	0
		[003]	0	0	0	0	0	$[003]_{12}$
		[012]	0	0	0	$[012]_{23}$	$[012]_{31}$	0
		[021]	0	0	0	0	0	$[021]_{12}$
		[102]	0	0	0	$[012]_{31}$	$-[012]_{23}$	0
		[201]	0	0	0	0	0	$[021]_{12}$
		[120]	0	0	0	$[300]_{23}$	$[300]_{31}$	0
		[210]	0	0	0	$-[300]_{31}$	$[300]_{23}$	0
		[111]	0	0	0	0	0	0
n=4	16	[400]	$[400]_{11}$	$[400]_{22}$	$[400]_{33}$	0	0	$-\frac{1}{8}\{[310]_{11}+3[130]_{11}\}$
		[040]	$[040]_{11}$	$[400]_{11}-[040]_{11}+[400]_{22}$	$[400]_{33}$	0	0	$\frac{1}{8}\{[130]_{11}+3[310]_{11}\}$
		[004]	$[004]_{11}$	$[004]_{11}$	$[004]_{33}$	0	0	0
		[013]	0	0	0	$[013]_{23}$	$[013]_{31}$	0
		[031]	0	0	0	$[031]_{23}$	$[031]_{31}$	0
		[103]	0	0	0	$-[013]_{31}$	$[013]_{23}$	0
		[301]	0	0	0	$-[031]_{31}$	$[031]_{23}$	0
		[130]	$[130]_{11}$	$-[130]_{11}$	0	0	0	$[400]_{11}+[040]_{11}-2[400]_{22}$
		[310]	$[310]_{11}$	$-[310]_{11}$	0	0	0	$[400]_{11}-3[040]_{11}+2[400]_{22}$
		[022]	$[202]_{22}$	$[202]_{11}$	$[202]_{33}$	0	0	$[022]_{12}$
		[202]	$[202]_{11}$	$[202]_{22}$	$[202]_{33}$	0	0	$-[022]_{12}$
		[220]	$[400]_{11}+4[400]_{22}-3[040]_{11}$	$[400]_{11}-2[400]_{22}+3[040]_{11}$	$2[400]_{33}$	0	0	$-\frac{3}{4}\{[310]_{11}-[130]_{11}\}$
		[211]	0	0	0	$[031]_{23}$	$[031]_{31}$	0
		[121]	0	0	0	$-[031]_{31}$	$[031]_{23}$	0
		[112]	$-2[022]_{12}$	$2[022]_{12}$	0	0	0	$[202]_{11}-[202]_{22}$

TABLE VI (continued)

THE BRACKET SYMBOLS UP TO n = 4, FOR D_{2h}

		ij	11	22	33	23	31	12
n=0	3	[000]	$[000]_{11}$	$[000]_{22}$	$[000]_{33}$	0	0	0
n=1	3	[100]	0	0	0	$[100]_{23}$	0	0
		[010]	0	0	0	0	$[010]_{31}$	0
		[001]	0	0	0	0	0	$[001]_{12}$
n=2	12	[200]	$[200]_{11}$	$[200]_{22}$	$[200]_{33}$	0	0	0
		[020]	$[020]_{11}$	$[020]_{22}$	$[020]_{33}$	0	0	0
		[002]	$[002]_{11}$	$[002]_{22}$	$[002]_{33}$	0	0	0
		[011]	0	0	0	$[011]_{23}$	0	0
		[101]	0	0	0	0	$[101]_{31}$	0
		[110]	0	0	0	0	0	$[110]_{12}$
n=3	9	[300]	0	0	0	$[300]_{23}$	0	0
		[030]	0	0	0	0	$[030]_{31}$	0
		[003]	0	0	0	0	0	$[003]_{12}$
		[012]	0	0	0	0	$[012]_{31}$	0
		[021]	0	0	0	0	0	$[021]_{12}$
		[102]	0	0	0	$[102]_{23}$	0	0
		[201]	0	0	0	0	0	$[201]_{12}$
		[120]	0	0	0	$[120]_{23}$	0	0
		[210]	0	0	0	0	$[210]_{31}$	0
		[111]	0	0	0	0	0	0
n=4	27	[400]	$[400]_{11}$	$[400]_{22}$	$[400]_{33}$	0	0	0
		[040]	$[040]_{11}$	$[040]_{22}$	$[040]_{33}$	0	0	0
		[004]	$[004]_{11}$	$[004]_{22}$	$[004]_{33}$	0	0	0
		[013]	0	0	0	$[013]_{23}$	0	0
		[031]	0	0	0	$[031]_{23}$	0	0
		[103]	0	0	0	0	$[103]_{31}$	0
		[301]	0	0	0	0	$[301]_{31}$	0
		[130]	0	0	0	0	0	$[130]_{12}$
		[310]	0	0	0	0	0	$[310]_{12}$
		[022]	$[022]_{11}$	$[022]_{22}$	$[022]_{33}$	0	0	0
		[202]	$[202]_{11}$	$[202]_{22}$	$[202]_{33}$	0	0	0
		[220]	$[220]_{11}$	$[220]_{22}$	$[220]_{33}$	0	0	0
		[211]	0	0	0	$[211]_{23}$	0	0
		[121]	0	0	0	0	$[121]_{31}$	0
		[112]	0	0	0	0	0	$[112]_{12}$

TABLE VI (continued)

THE BRACKET SYMBOLS, UP TO n = 4, FOR D_{3i}

(C_2 along k_1)

	ij	11	22	33	23	31	12
n=0	2 [000]	$[000]_{11}$	$[000]_{11}$	$[000]_{33}$	0	0	0
n=1	2 [100]	0	0	0	$[100]_{23}$	0	0
	[010]	0	0	0	0	$[100]_{23}$	0
	[001]	0	0	0	0	0	$[001]_{12}$
n=2	8 [200]	$[200]_{11}$	$[200]_{22}$	$[200]_{33}$	$[200]_{23}$	0	0
	[020]	$[200]_{22}$	$[200]_{11}$	$[200]_{33}$	$-[200]_{23}$	0	0
	[002]	$[002]_{11}$	$[002]_{11}$	$[002]_{33}$	0	0	0
	[011]	$[011]_{11}$	$-[011]_{11}$	0	$[011]_{23}$	0	0
	[101]	0	0	0	0	$[011]_{23}$	$[011]_{11}$
	[110]	0	0	0	0	$2[200]_{23}$	$[200]_{11}-[200]_{22}$
n=3	6 [300]	0	0	0	$[300]_{23}$	0	0
	[030]	0	0	0	0	$[300]_{23}$	$[030]_{12}$
	[003]	0	0	0	0	0	$[003]_{12}$
	[012]	0	0	0	0	$[012]_{31}$	0
	[021]	0	0	0	0	$[021]_{31}$	$[021]_{12}$
	[102]	0	0	0	$[012]_{31}$	0	0
	[201]	0	0	0	0	$-[021]_{31}$	$[021]_{12}$
	[120]	0	0	0	$[300]_{23}$	0	0
	[210]	0	0	0	0	$[300]_{23}$	$-3[030]_{12}$
	[111]	0	0	0	$-2[021]_{31}$	0	0
n=4	1 [400]	$[400]_{11}$	$[400]_{22}$	$[400]_{33}$	$[400]_{23}$	0	0
	[040]	$[040]_{11}$	$[400]_{11}+[400]_{22}-[040]_{11}$	$[400]_{33}$	$[040]_{23}$	0	0
	[004]	$[004]_{11}$	$[004]_{11}$	$[004]_{33}$	0	0	0
	[013]	$[013]_{11}$	$-[013]_{11}$	0	$[013]_{23}$	0	0
	[031]	$[031]_{11}$	$[031]_{11}$	$[031]_{33}$	$[031]_{23}$	0	0
	[103]	0	0	0	0	$[013]_{23}$	$[013]_{11}$
	[301]	0	0	0	0	$[031]_{23}$	$[301]_{12}$
	[130]	0	0	0	0	$3[400]_{23}+[040]_{23}$	$[400]_{11}-2[400]_{22}+[040]_{11}$
	[310]	0	0	0	0	$-[400]_{23}-3[040]_{23}$	$[400]_{11}+2[400]_{22}-3[040]_{11}$
	[022]	$[202]_{22}$	$[202]_{11}$	$[202]_{33}$	$-[202]_{23}$	0	0
	[202]	$[202]_{11}$	$[202]_{22}$	$[202]_{33}$	$[202]_{23}$	0	0
	[220]	$[400]_{11}+4[400]_{22}-3[040]_{11}$	$[400]_{11}-2[400]_{22}+3[040]_{11}$	$2[400]_{33}$	$-3\{[400]_{23}+[040]_{23}\}$	0	0
	[211]	$-3[031]_{11}+4[301]_{12}$	$-3[031]_{11}+2[301]_{12}$	$-3[031]_{33}$	$[031]_{23}$	0	0
	[121]	0	0	0	0	$[031]_{23}$	$[301]_{12}$
	[112]	0	0	0	0	$2[202]_{23}$	$[202]_{11}-[202]_{22}$

TABLE VI (continued)

THE BRACKET SYMBOLS UP TO n = 4, FOR D_{4h}

		ij	11	22	33	23	31	12
n=0	2	[000]	$[000]_{11}$	$[000]_{11}$	$[000]_{33}$	0	0	0
n=1	2	[100]	0	0	0	$[100]_{23}$	0	0
		[010]	0	0	0	0	$[100]_{23}$	0
		[001]	0	0	0	0	0	$[001]_{12}$
n=2	7	[200]	$[200]_{11}$	$[200]_{22}$	$[200]_{33}$	0	0	0
		[020]	$[200]_{22}$	$[200]_{11}$	$[200]_{33}$	0	0	0
		[002]	$[002]_{11}$	$[002]_{11}$	$[002]_{33}$	0	0	0
		[011]	0	0	0	$[011]_{23}$	0	0
		[101]	0	0	0	0	$[011]_{23}$	0
		[110]	0	0	0	0	0	$[110]_{12}$
n=3	5	[300]	0	0	0	$[300]_{23}$	0	0
		[030]	0	0	0	0	$[300]_{23}$	0
		[003]	0	0	0	0	0	$[003]_{12}$
		[012]	0	0	0	0	$[012]_{31}$	0
		[021]	0	0	0	0	0	$[201]_{12}$
		[102]	0	0	0	$[012]_{31}$	0	0
		[201]	0	0	0	0	0	$[201]_{12}$
		[120]	0	0	0	$[120]_{23}$	0	0
		[210]	0	0	0	0	$[120]_{23}$	0
		[111]	0	0	0	0	0	0
n=4	15	[400]	$[400]_{11}$	$[400]_{22}$	$[400]_{33}$	0	0	0
		[040]	$[400]_{22}$	$[400]_{11}$	$[400]_{33}$	0	0	0
		[004]	$[004]_{11}$	$[004]_{11}$	$[004]_{33}$	0	0	0
		[013]	0	0	0	$[013]_{23}$	0	0
		[031]	0	0	0	$[031]_{23}$	0	0
		[103]	0	0	0	0	$[013]_{23}$	0
		[301]	0	0	0	0	$[031]_{23}$	0
		[130]	0	0	0	0	0	$[130]_{12}$
		[310]	0	0	0	0	0	$[130]_{12}$
		[022]	$[202]_{22}$	$[202]_{11}$	$[202]_{33}$	0	0	0
		[202]	$[202]_{11}$	$[202]_{22}$	$[202]_{33}$	0	0	0
		[220]	$[220]_{11}$	$[220]_{11}$	$[220]_{33}$	0	0	0
		[211]	0	0	0	$[211]_{23}$	0	0
		[121]	0	0	0	0	$[211]_{23}$	0
		[112]	0	0	0	0	0	$[112]_{12}$

TABLE VI (continued)

THE BRACKET SYMBOLS UP TO n=4, FOR D_{6h}

		ij	11	22	33	23	31	12
n=0	2	[000]	$[000]_{11}$	$[000]_{11}$	$[000]_{33}$	0	0	0
n=1	2	[100]	0	0	0	$[100]_{23}$	0	0
		[010]	0	0	0	0	$[100]_{23}$	0
		[001]	0	0	0	0	0	$[001]_{12}$
n=2	6	[200]	$[200]_{11}$	$[200]_{22}$	$[200]_{33}$	0	0	0
		[020]	$[200]_{22}$	$[200]_{11}$	$[200]_{33}$	0	0	0
		[002]	$[002]_{11}$	$[002]_{11}$	$[002]_{33}$	0	0	0
		[011]	0	0	0	$[011]_{23}$	0	0
		[101]	0	0	0	0	$[011]_{23}$	0
		[110]	0	0	0	0	0	$[200]_{11}-[200]_{22}$
n=3	3	[300]	0	0	0	$[300]_{23}$	0	0
		[030]	0	0	0	0	$[300]_{23}$	0
		[003]	0	0	0	0	0	$[003]_{12}$
		[012]	0	0	0	0	$[012]_{31}$	0
		[021]	0	0	0	0	0	$[021]_{12}$
		[102]	0	0	0	$[012]_{31}$	0	0
		[201]	0	0	0	0	0	$[021]_{12}$
		[120]	0	0	0	$[300]_{23}$	0	0
		[210]	0	0	0	0	$[300]_{23}$	0
		[111]	0	0	0	0	0	0
n=4	12	[400]	$[400]_{11}$	$[400]_{22}$	$[400]_{33}$	0	0	0
		[040]	$[040]_{11}$	$[400]_{11}-[040]_{11}+[400]_{22}$	$[400]_{33}$	0	0	0
		[004]	$[004]_{11}$	$[004]_{11}$	$[004]_{33}$	0	0	0
		[013]	0	0	0	$[013]_{23}$	0	0
		[031]	0	0	0	$[031]_{23}$	0	0
		[103]	0	0	0	0	$[013]_{23}$	0
		[301]	0	0	0	0	$[031]_{23}$	0
		[130]	0	0	0	0	0	$[400]_{11}+[040]_{11}-2[400]_{22}$
		[310]	0	0	0	0	0	$[400]_{11}-3[040]_{11}+2[400]_{22}$
		[022]	$[202]_{22}$	$[202]_{11}$	$[202]_{23}$	0	0	0
		[202]	$[202]_{11}$	$[202]_{22}$	$[202]_{33}$	0	0	0
		[220]	$[400]_{11}+4[400]_{22}-3[040]_{11}$	$[400]_{11}-2[400]_{22}+3[040]_{11}$	$2[400]_{33}$	0	0	0
		[211]	0	0	0	$[031]_{23}$	0	0
		[121]	0	0	0	0	$[031]_{23}$	0
		[112]	0	0	0	0	0	$[202]_{11}-[202]_{22}$

TABLE VI (continued)

THE BRACKET SYMBOLS UP TO n = 4, FOR T_h

		ij	11	22	33	23	31	12
n=0	1	[000]	$[000]_{11}$	$[000]_{11}$	$[000]_{11}$	0	0	0
n=1	1	[100]	0	0	0	$[100]_{23}$	0	0
		[010]	0	0	0	0	$[100]_{23}$	0
		[001]	0	0	0	0	0	$[100]_{23}$
n=2	4	[200]	$[200]_{11}$	$[200]_{22}$	$[200]_{33}$	0	0	0
		[020]	$[200]_{33}$	$[200]_{11}$	$[200]_{22}$	0	0	0
		[002]	$[200]_{22}$	$[200]_{33}$	$[200]_{11}$	0	0	0
		[011]	0	0	0	$[011]_{23}$	0	0
		[101]	0	0	0	0	$[011]_{23}$	0
		[110]	0	0	0	0	0	$[011]_{23}$
n=3	3	[300]	0	0	0	$[300]_{23}$	0	0
		[030]	0	0	0	0	$[300]_{23}$	0
		[003]	0	0	0	0	0	$[300]_{23}$
		[012]	0	0	0	0	$[012]_{31}$	0
		[021]	0	0	0	0	0	$[102]_{23}$
		[102]	0	0	0	$[102]_{23}$	0	0
		[201]	0	0	0	0	0	$[012]_{31}$
		[120]	0	0	0	$[012]_{31}$	0	0
		[210]	0	0	0	0	$[102]_{23}$	0
		[111]	0	0	0	0	0	0
n=4	9	[400]	$[400]_{11}$	$[400]_{22}$	$[400]_{33}$	0	0	0
		[040]	$[400]_{33}$	$[400]_{11}$	$[400]_{22}$	0	0	0
		[004]	$[400]_{22}$	$[400]_{33}$	$[400]_{11}$	0	0	0
		[013]	0	0	0	$[013]_{23}$	0	0
		[031]	0	0	0	$[031]_{23}$	0	0
		[103]	0	0	0	0	$[031]_{23}$	0
		[301]	0	0	0	0	$[013]_{23}$	0
		[130]	0	0	0	0	0	$[013]_{23}$
		[310]	0	0	0	0	0	$[031]_{23}$
		[022]	$[022]_{11}$	$[022]_{22}$	$[022]_{33}$	0	0	0
		[202]	$[022]_{33}$	$[022]_{11}$	$[022]_{22}$	0	0	0
		[220]	$[022]_{22}$	$[022]_{33}$	$[022]_{11}$	0	0	0
		[211]	0	0	0	$[211]_{23}$	0	0
		[121]	0	0	0	0	$[211]_{23}$	0
		[112]	0	0	0	0	0	$[211]_{23}$

TABLE VI (continued)

THE BRACKET SYMBOLS UP TO n = 4, FOR O_h

		ij	11	22	33	23	31	12
n=0	1	[000]	$[000]_{11}$	$[000]_{11}$	$[000]_{11}$	0	0	0
n=1	1	[100]	0	0	0	$[100]_{23}$	0	0
		[010]	0	0	0	0	$[100]_{23}$	0
		[001]	0	0	0	0	0	$[100]_{23}$
n=2	3	[200]	$[200]_{11}$	$[200]_{22}$	$[200]_{22}$	0	0	0
		[020]	$[200]_{22}$	$[200]_{11}$	$[200]_{22}$	0	0	0
		[002]	$[200]_{22}$	$[200]_{22}$	$[200]_{11}$	0	0	0
		[011]	0	0	0	$[011]_{23}$	0	0
		[101]	0	0	0	0	$[011]_{23}$	0
		[110]	0	0	0	0	0	$[011]_{23}$
n=3	2	[300]	0	0	0	$[300]_{23}$	0	0
		[030]	0	0	0	0	$[300]_{23}$	0
		[003]	0	0	0	0	0	$[300]_{23}$
		[012]	0	0	0	0	$[012]_{31}$	0
		[021]	0	0	0	0	0	$[012]_{31}$
		[102]	0	0	0	$[012]_{31}$	0	0
		[201]	0	0	0	0	0	$[012]_{31}$
		[120]	0	0	0	$[012]_{31}$	0	0
		[210]	0	0	0	0	$[012]_{31}$	0
		[111]	0	0	0	0	0	0
n=4	6	[400]	$[400]_{11}$	$[400]_{22}$	$[400]_{22}$	0	0	0
		[040]	$[400]_{22}$	$[400]_{11}$	$[400]_{22}$	0	0	0
		[004]	$[400]_{22}$	$[400]_{22}$	$[400]_{11}$	0	0	0
		[013]	0	0	0	$[013]_{23}$	0	0
		[031]	0	0	0	$[013]_{23}$	0	0
		[103]	0	0	0	0	$[013]_{23}$	0
		[301]	0	0	0	0	$[013]_{23}$	0
		[130]	0	0	0	0	0	$[013]_{23}$
		[310]	0	0	0	0	0	$[013]_{23}$
		[022]	$[022]_{11}$	$[022]_{22}$	$[022]_{22}$	0	0	0
		[202]	$[022]_{22}$	$[022]_{11}$	$[022]_{22}$	0	0	0
		[220]	$[022]_{22}$	$[022]_{22}$	$[022]_{11}$	0	0	0
		[211]	0	0	0	$[211]_{23}$	0	0
		[121]	0	0	0	0	$[211]_{23}$	0
		[112]	0	0	0	0	0	$[211]_{23}$

C. EXPERIMENTAL PART

1. Equipment

The holder with Cardan suspension mentioned in the previous report was completed. In this holder, the bismuth sample is encased in a lucite capsule with copper gallium well electrodes separated by a thin mica sheet. The connections were made with two small silver wires in spiral form in order that the rotation of the capsule may be almost torque free. The MR effect of silver wire was checked to be negligible in the range of the magnetic fields used.

The sample wire can be rotated around its own axis; the angle of this rotation is denoted by θ . It also can be rotated around two mutually perpendicular axes. One of these axes has a fixed position perpendicular to the magnetic field and is called the ϕ axis; the other axis ψ is perpendicular to both the θ and ϕ axes. Thus ψ represents the angle between the sample and the ϕ axis. The sample holder permits turning around these axes within a 1-1/2-inch gap between the magnet poles. (See Figure 1).

In order to enable us to detect slight deviations from the law $\Delta\rho/\rho = BH^2$ accurately, it was necessary to calibrate the magnetic field with more precision than $\pm 5\%$. The new calibration of the same magnet was done with the cooperation of Dr. W. C. Parkinson of this laboratory by the method of proton spin reasonance. This method is capable of calculating the values of the magnetic field H accurately to the fifth digit, which is more than needed since the current reading was only accurate to about 0.5 %. Therefore all calibration errors will be due to the readings of the magnet current I. Graphical analysis of the dependence of H on I showed

$$H = 199.5 I \qquad (I \leq 6 \text{ amp})$$

compared to the old calibration

$$H = 196 I - 10 \qquad (\pm 5\%)$$

2. Materials

The bismuth used was from the same sources described in Report No. 2. Besides the samples prepared by the drawing method, some samples prepared by coating bismuth on small glass tubing, wire tried for the MR effect.

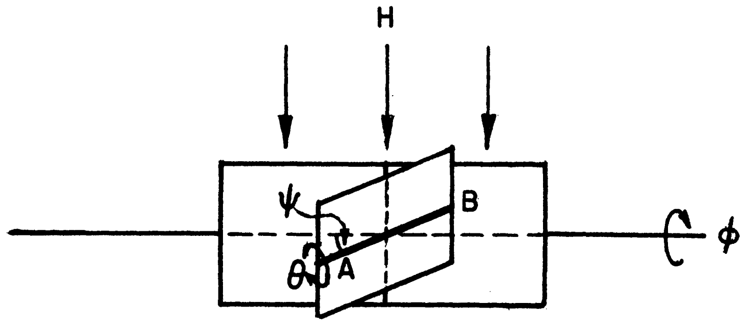

Fig. 1a. Mounting Diagram of Wire AB in Cardan Suspension with Angles θ, ϕ, and ψ.

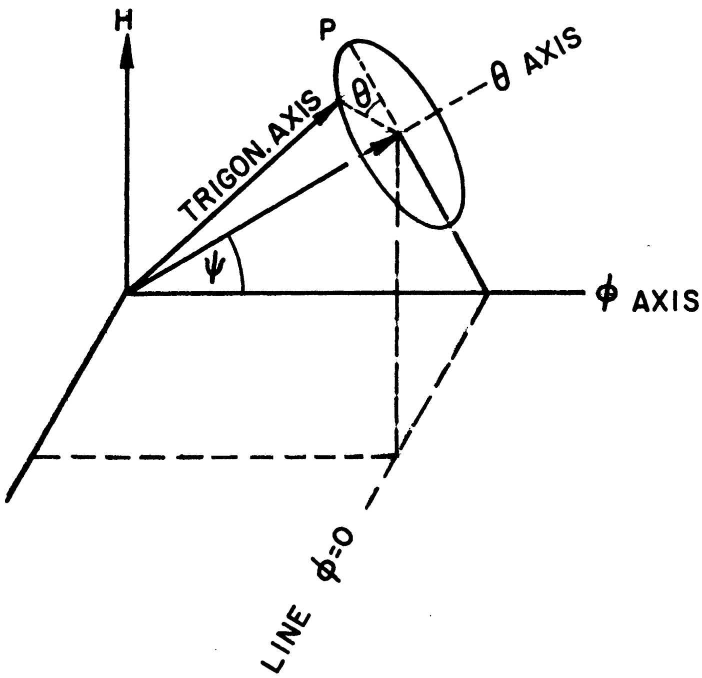

Fig. 1b. The Trigonal Axis is Set, During Measurement, to Point at P.

3. Measurements

a. Dependence of the MR Effect on Orientation and on H. Since the theoretical development requires many measurements with various orientations, in order to find the fundamental constants of the bismuth crystal, the MR effect was measured for various ψ in steps of 10° from 0 to 90°, and at various ϕ in steps of 20° from 0 to 360°. The angle θ was to set the trigonal axis, the wire axis and the ϕ axis in the same plane. This would make possible to align the trigonal axis along the ϕ axis. As reported previously the trigonal axis can be determined by looking at the cleavage plane under a reflection microscope. However, in this way the angle between the trigonal axis and the wire axis is only determined to within ± 2°, consequently the plane containing the two axes cannot be determined with sufficient accuracy as required to set the angle θ. This plane is determined instead by using the criterion that if the θ and ϕ axes coincide (ψ=0) then $\frac{\Delta\rho}{\rho}$ is a maximum as a function of θ or ϕ when the trigonal axis is in the plane of H and the current through the sample i.

From the fact proved in the previous report that

$$\left(\frac{\Delta\rho}{\rho}\right)_{+H} = \left(\frac{\Delta\rho}{\rho}\right)_{-H} ,$$

it was expected that the measurements at ϕ = 90° or 270° at any ψ would give the same value of $\frac{\Delta\rho}{\rho}$. The values were found to be the same within experimental error, provided i is sufficiently small (in our case < 20 ma). The value

$$\frac{1}{2}\left\{\left(\frac{\Delta\rho}{\rho}\right)_{\phi=90} + \left(\frac{\Delta\rho}{\rho}\right)_{\phi=270}\right\}$$

was used to "normalize " the measurements done on different occasions on the same sample. (See Fig. 2) It was found expedient to use a magnetic field of 594 gauss. This would insure

$$\left(\frac{\Delta\rho}{\rho}\right)_{+H} = \left(\frac{\Delta\rho}{\rho}\right)_{-H}$$

and yet would cause enough deflection in the galvanometer, with i from 2 to 20 ma.

In order to calculate the fundamental constants of bismuth crystals one must determine beside the position of the trigonal axis with respect to the directions of H and i, the position of a binary axis and the resistivity of the sample. It has been tried to find the binary axis by an etching method. The technique has not yet been successful. The determination of the resistivity involves breaking up the sample to average the cross-sectional area viewed under a microscope, and thus will have to wait until the binary axis is determined. A few test samples were tried and the resistivity was found to be of the order of $100 \times 10^{-6}\ \Omega$ cm.

The data of measurements will be kept for later evaluation. A family of curves representing a typical $\frac{\Delta\rho}{\rho}$ measurement in various directions is shown in Fig. 2. Fig. 3 shows the set of measurements for one particular sample which exhibits no shift of the maximum and minimum points. The curves show accurately sinusoidal shapes, indicating that if $(\Delta\rho/\rho)^{-1/2}$ were plotted as a function of direction, an ellipsoid would result. This manner of plotting will be discussed with the theory of the next report. At the closing of the report it was tried to raise the magnetic field intensity enough to show the next higher power term, or

$$\frac{\Delta\rho}{\rho} = BH^2 - CH^4$$

This was done with the sample in the position $\Theta = \psi = 0$. From the above relation it is seen that $\Delta\rho/\rho H^2$ should be plotted versus H^2. A typical plot is shown in Fig. 4, from the data given in Table 1. Note the expanded ordinate scale.

This plot shows a straight line relation over its major part, permitting the determination of B and C. The deviation of the first point is within the limits of error, which are larger on the left side of this plot than on the right. Table 2 gives values of B and C for a few of the samples measured.

b. Singleness of Crystals. To be sure of our samples being single crystals, we studied the direction of the cleavage planes after successive breaking while the sample was held fixed under the microscope. It was found that if the sample looked continuously smooth by the naked eyes (i.e., no cracks, no bubbles when reflecting light) then it had constant direction of the cleavage plane. Our samples are now being taken from the center part of a long piece; the end parts are broken and the cleavage planes checked to be the same. Only single crystals are used for measurements as reported under a).

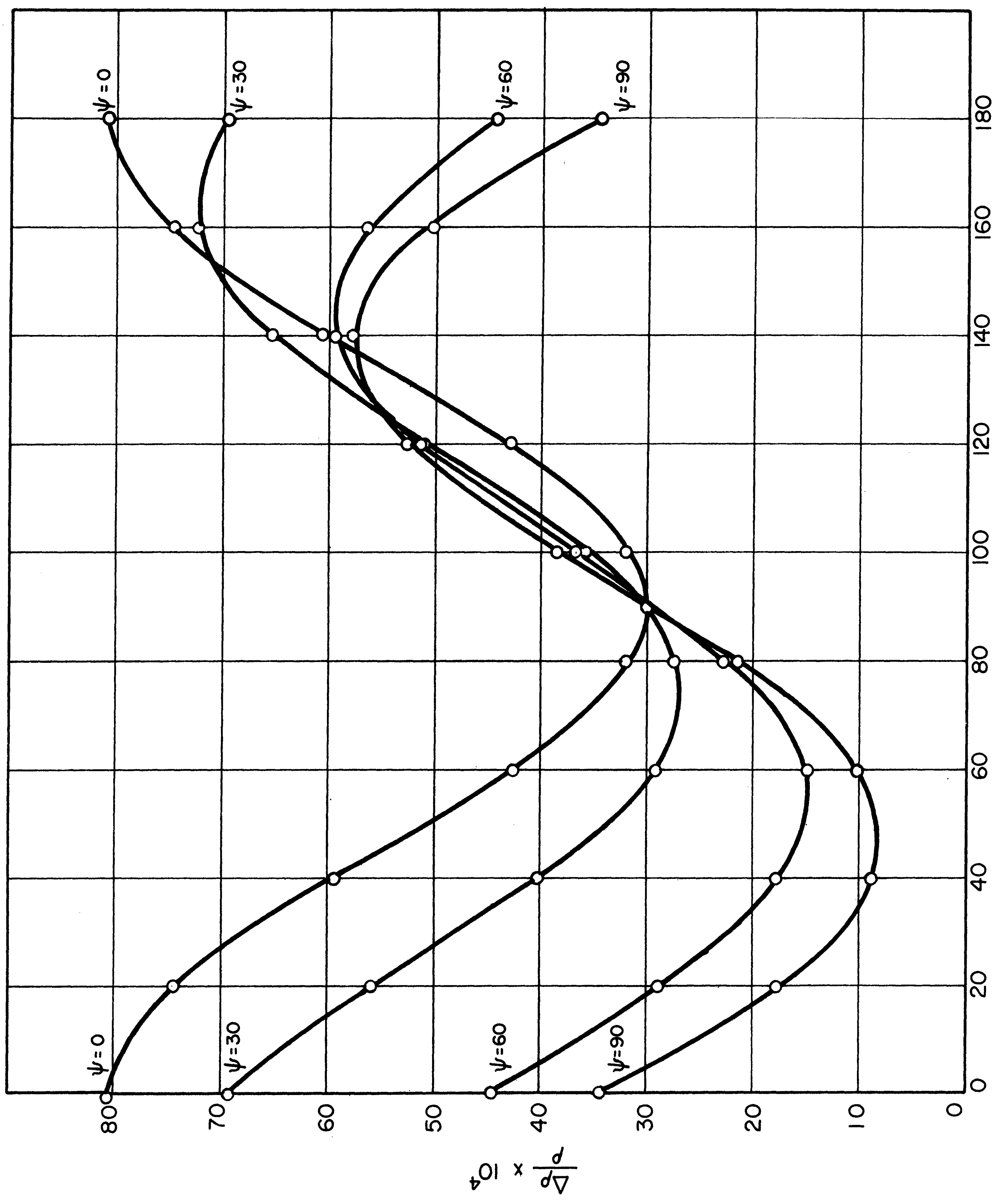

Fig. 2. Sample No. 1 in Table VII.

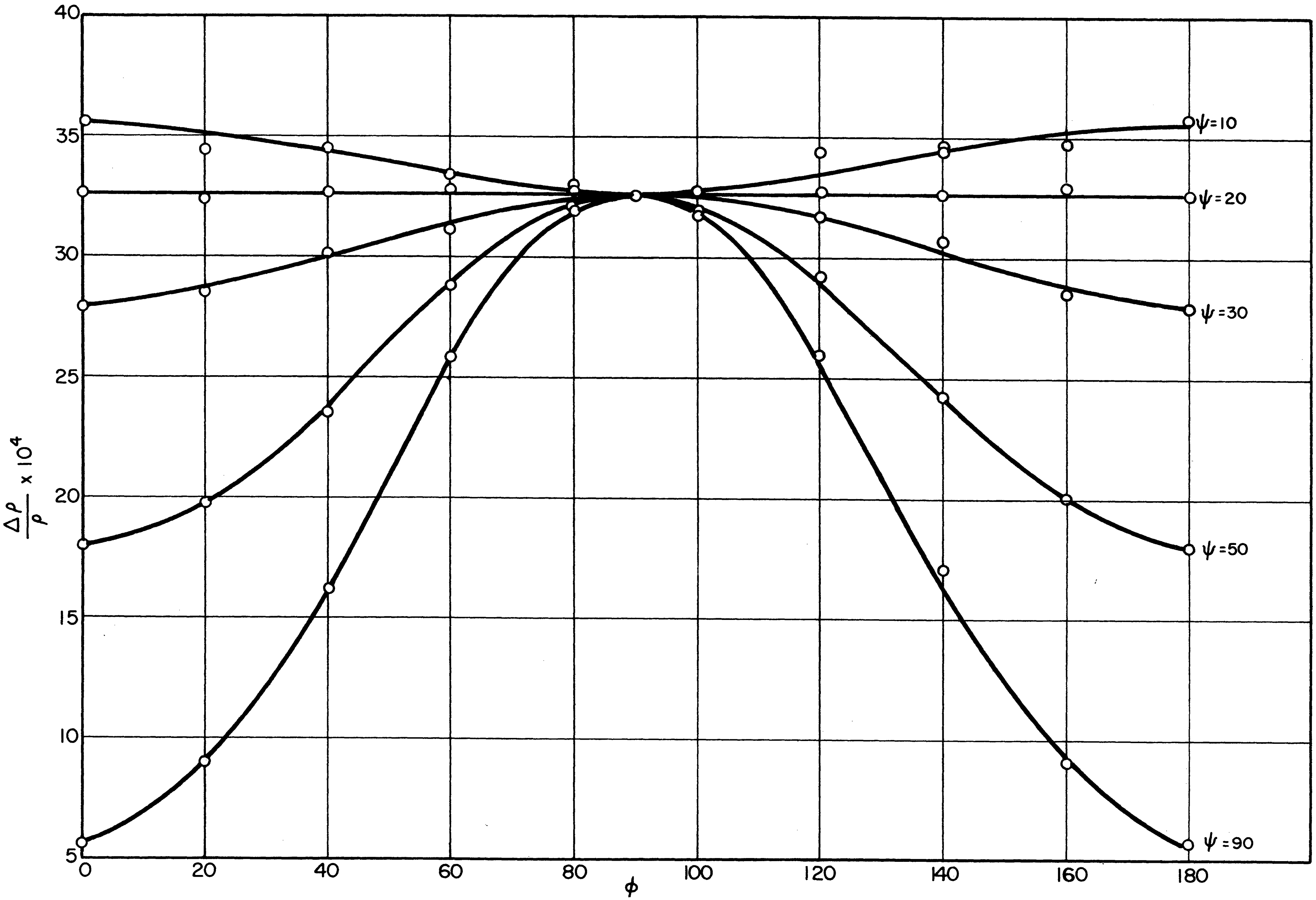

Fig. 3. Sample No. 3 in Table VIII.

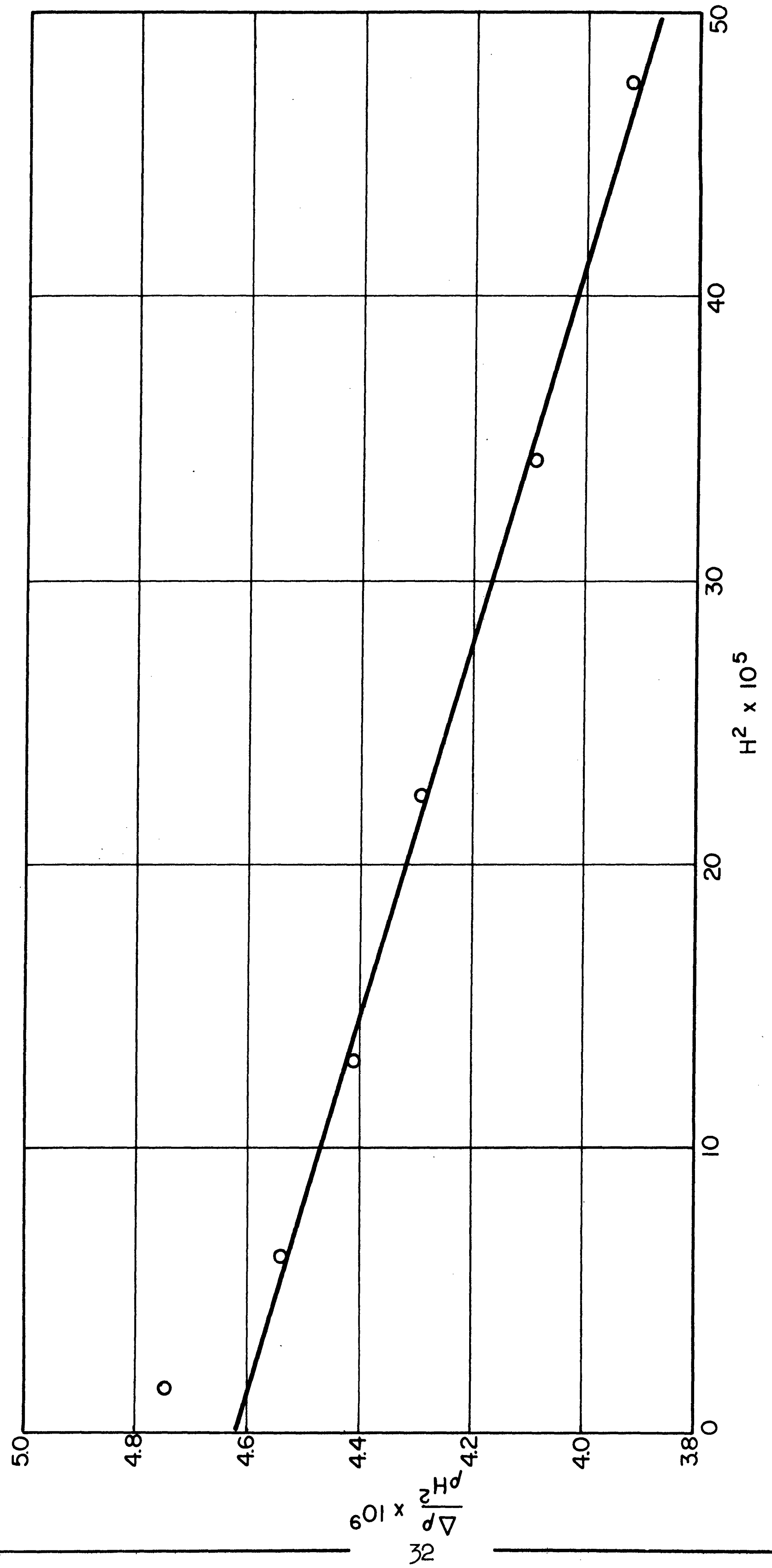
0
10
20
30
40
50
$H^2 \times 10^5$
5.0
4.8
4.6
4.4
4.2
4.0
3.8
$\frac{\Delta p}{\rho H^2} \times 10^9$

Fig. 4

TABLE VII

DATA FOR PLOTTING $\frac{\Delta\rho}{\rho H^2}$ vs H^2 IN FIG. 4, TAKEN

FROM MEASUREMENTS ON SAMPLE NO. 3 IN TABLE VIII

H	$\frac{\Delta\rho}{\rho} \times 10^4$	$H^2 \times 10^{-5}$	$\frac{\Delta\rho}{\rho H^2} \times 10^9$
398	7.53	1.584	4.75
786	28.12	6.199	4.54
1144	57.90	13.11	4.41
1500	96.60	22.50	4.29
1850	140.0	34.25	4.09
2180	186.0	47.52	3.92

TABLE VIII

THE CONSTANTS B,C IN THE RELATION $\frac{\Delta\rho}{\rho H^2} = B - CH^2$

No.	Trigonal Axis From Wire Axis	B x 10^9 $\phi=\psi=0$	C x 10^{16} $\phi=\psi=0$	B x 10^9 $\phi=\psi=90°$	C x 10^9 $\phi=\psi=90°$	Remarks
1	To be determined	11.8±0.1	7	4.45±0.1	0.8	99.8 % Bi Zone Treated
2	18 ± 2°	12.98±0.05	6.06±0.1	2.8±0.3	-	99.8 % Bi Zone Treated
3	0 ± 4°	4.62±0.05	1.4±0.1	-	-	Fitzpatrick Bi not zone treated
4	2 ± 2°	∼ 20	-	∼ 8.3		Fitzpatrick Bi not zone treated
5	-	5.0±0.2	3±0.5	-	-	Coated Bi 99.8%.

The samples made by drawing Baker and Adamson Bi were found to be as good as those drawn from Fitzpatrick Bi in being single crystals. The zone melting of a Bi sample in a transverse magnetic field of about 6,000 gausses did not influence the orientation of the trigonal axis, nor did it insure the singleness of crystals. In fact it was frequently found that new cracks were introduced.

c. Bismuth Coating on Glass Tubes. Tubes were drawn to have outer diameters of about 0.2 mm. They were placed horizontally at various heights above a porcelain crucible with melting bismuth in high vacuum. The bismuth used was from the 99.8% pure Baker and Adamson lot. It was found that:

(1) The coating depends on the height. At some high temperature the coating was grainy and not very conductive up to the height of about 1 cm above the melt, and was smooth, conducting, at higher levels. The boundary was sharply noticeable. However, at lower temperature the boundary was lower and at a temperature close to the melting point of bismuth it disappeared.

(2) The coating is better if the evaporation is done at lower temperature during a longer time.

3) The vacuum should be better than 10^{-5} mm. This was done with a mercury diffusion pump and a liquid air trap.

(4) The glass tube should not be too hot. The temperature was not determined, however. This may well be connected with the results mentioned under (1).

(5) Most of the samples obtained this way exhibited very little or no angular variation in the $\frac{\Delta\rho}{\rho}$ measurement. This shows that the sample obtained this way is poly-crystalline or perhaps amorphous. The constant B in the equation $\frac{\Delta\rho}{\rho} = BH^2$ for a few samples was found to be between 4.5×10^{-9} and 6.0×10^{-9}, which is of the same order of magnitude as the average of B- values for pure Bi wires reported in previous reports, possibly somewhat smaller.

4. Conclusions

The technique for checking singleness of crystals was improved. The wires were measured in all orientations with respect to H by means of a Cardan suspension. The results indicate an "ellipsoid of magneto resistance," but detailed interpretation is deferred until the next report when the theory will be further worked out.

Accurate measurements at fields up to 2500 gauss show a term in Bi proprotional to H^4.

Efforts towards coating a thin Bi film on glass were successful in establishing conditions for obtaining a smooth, adherent conducting film.

D. PROGRAM FOR NEXT INTERVAL

1. Theoretical

In the further development of the theory, an effort will be made toward discussing completely the MR ellipsoid, and toward discussing other properties of the bracket symbols, for example their temperature dependence.

2. Experimental

Certain aging effects of bismuth MR will be studied. Further work will be done on the MR of thin Bi films. The range of H will be extended to the order of 10,000 gauss. Consideration will be given to work at lower temperatures and to the design of ac measuring equipment using very low measuring currents.

E. PERSONNEL

Of the persons mentioned in the previous report, the following do no longer work on this project: Miss K. Hanchon, Mr. B. Crane (temporary), and Mr. Alsaqqar. At the end of the summer, Mr. S. H. Yeh worked for approximately six weeks on the problem of the thin films, Dr. T. S. Change looked briefly into some theoretical aspects of the azimuth dependence of the MR effect. These two men had only a limited period of time available since they had to leave Ann Arbor with the beginning of the fall term. Mrs. Suits is still here, helping with some theoretical work.

In the period of June, July, August, and September, 1954, the major part of the theoretical work reported was done by Mr. Kao and Dr. Katz, whereas the experimental work other than the thin films was done by Mr. Tantraporn and Mr. Patterson.